CrystEngComm

Accepted Manuscript

This article can be cited before page numbers have been issued, to do this please use: P. S. Hariharan, P. Gayathri, A. Kundu, S. Karthikeyan, D. Moon and P. P. Anthony, *CrystEngComm*, 2017, DOI: 10.1039/C7CE01867C.

ROYAL SOCIETY OF CHEMISTRY

rsc.li/crystengcomm

View Article Online
DOI: 10.1039/C7CE01867C

Journal Name

ARTICLE

Synthesis of tunable, red fluorescent aggregation enhanced emissive organic fluorophores: Stimuli responsive high contrast off-on fluorescence switching

Received 00th January 20xx,
Accepted 00th January 20xx

DOI: 10.1039/x0xx00000x

www.rsc.org/

Palamarneri Sivaraman Hariharan,[a] Parthasarathy Gayathri,[a] Anu Kundu,[a] Subramanian Karthikeyan,[b] Dohyun Moon*[c] and Savarimuthu Philip Anthony*[a]

Triphenylamine (TPA) and N-methylbarbituric acid/indanedione based donor-acceptor derivatives were synthesized and demonstrated molecular conformation and packing dependent tunable fluorescence from yellow to red in the solid state. TPA with N-methylbarbituric acid (BA-1) showed bright yellow fluorescence (λ_{max} = 550 nm, Φ_f = 22.8 %) whereas OCH_3 substitution at phenyl rings of TPA, (BA-2 and BA-3) produced strong red (λ_{max} = 602 nm, Φ_f = 41.1 %) and orange fluorescent solids (λ_{max} = 582 nm, Φ_f = 19.1 %). Indanedione acceptor dyes exhibited red to deep red fluorescence. ID-1 showed red fluorescence at 604 nm (Φ_f = 17.7 %) whereas ID-2 and ID-3 showed fluorescence at 611 (Φ_f = 19.4 %) and 636 nm (Φ_f = 14.1 %) in the solid state. Solid state structural analysis revealed alteration of molecular conformation and packing by OCH_3 substitution and lead to tunable fluorescence. BA and ID compounds showed turn-off/substantially reduced fluorescence intensity upon hard crushing (Φ_f = 1.2 to 3.1 %). Interestingly, heating of BA and ID crushed powders lead to turn-on/significant enhancement of fluorescence intensity (Φ_f = 5.6 to 22.5 %). Powder X-ray diffraction (PXRD) studies indicated the conversion of crystalline to amorphous and amorphous to crystalline phase by hard crushing and heating. The reversible conversion of crystalline to amorphous phase was responsible for fluorescence switching of BA and ID. Computational studies have been performed to get the insight on the energy level modulation upon changing of the molecular conformation. Thus we have presented facile preparation of strong red fluorescent dyes with high contrast stimuli responsive reversible dark and bright fluorescence switching in the solid state.

Introduction

Switching and tuning of organic solid state fluorescence have received strong interest in recent years because of their application potential in various optoelectronic devices including sensors, displays, data storage, optical switches and security inks.[1,2] Organic fluorophore conformation, packing and intermolecular interactions plays important role to make the molecules to emit in the solid state as well as switching and tuning of fluorescence.[3] For example, strongly fluorescent π-conjugated fluorophores become non-fluorescent in the solid state due to the aggregation caused fluorescence quenching (ACQ). In contrast, non-planar fluorophore that prevents close packing in the solid state produced aggregation enhanced emission (AEE) in the solid state via rigidification of fluorophore by weak intermolecular interactions.[4] Further, subtle alteration of molecular conformation, packing and intermolecular interactions via substituent or by applying external stimuli such as mechanical force, heat and solvent exposure lead to tunable and switchable solid state fluorescence.[3,5-8] Often, conformationally twisted tetraphenylpyrene, pyrene- and anthracene-based liquid crystals, cyanostilbene and triphenylamine derivatives have been utilized to develop reversible fluorescence switching with external force.[9] Fluorescence-phosphorescence dual mechanoluminescence at room temperature has been reported for terphenyl-dioxaborolane derivative.[10] Substitution controlled stacking mode dependent mechanofluorochromism was observed in 3-aryl-2-cyano acrylamide derivatives in the solid state.[11] Temperature induced reversible phase changes in aromatic amine, terpyridine and excited state intramolecular proton transfer (ESIPT) compounds produced reversible fluorescence switching.[12] Cyano-substituted oligo(*p*-phenylene vinylene) derivative exhibited crystalline to crystalline phase transition when grinding at high temperature and exhibited fluorescence switching.[13] However, compared to external stimuli induced mechanofluorochromism, relatively less number of organic materials showed high-contrast on-off fluorescence switching.[2a, 12b,14] For example, acceptor-donor-acceptor triad based on dicyanodistyrylbenzene exhibited high contrast reversible on-off fluorescence by applying external force.[15]

[a] Department of Chemistry, School of Chemical & Biotechnology, SASTRA University, Thanjavur-613401, Tamil Nadu, India. E-mail: philip@biotech.sastra.edu
[b] Department of Chemistry, Kalasalingam University, Krishnan Kovil–626126, India
[c] Beamline Department, Pohang Accelerator Laboratory, 80 Jigokro-127beongil, Nam-gu, Pohang, Gyeongbuk, Korea. E-mail: dmoon@postech.ac.kr
[d] Electronic Supplementary Information (ESI) available: Synthetic scheme, NMR data, fluorescence spectra, crystal structures, PXRD pattern.. See DOI: 10.1039/x0xx00000x

View Article Online
DOI: 10.1039/C7CE01867C

Diphenylquinoxaline core with anthracene showed heat responsive on-off fluorescence switching in the solid state.[16] A unique piezochromic fluorescent organic crystals with pressure dependent reversible off-on fluorescence switching has been reported recently.[17]

The non-planar propeller shape, synthetic tailorability and good optoelectronic properties of triphenylamine (TPA) has been exploited for fabricating organic materials for dye sensitized solar cell, organic light emitting diode (OLED), field effect transistor, sensor, solid state fluorescent and smart fluorescent materials.[18] The conformational robustness and twisted propeller core of TPA prevented close packing of fluorophore in the solid state and often produced AEE and mechanofluorochromism.[19] Self-reversible and reversible mechanofluoro-chromism, tunable solid state fluorescence via polymorphism, self-erasable and rewritable fluorescent platforms have been demonstrated using TPA by tailoring acceptor structure, substituent position and halochromic functionality.[20] In this manuscript, we report the facile synthesis of red emissive, high contrast off-on fluorescence switching triphenylamine derivatives and molecular conformation and packing dependent tunable fluorescence from yellow to red in the solid state. BA-1 showed yellow fluorescence whereas methoxy substituted BA-2 and BA-3 produced red and orange fluorescent solids (Table 1). ID derivatives (ID-1 to 3) showed red to deep red fluorescence in the solid state (Table 1). Absolute quantum yield measurement confirmed strong fluorescence of these compounds in the solid state (Table 1). Interestingly, all derivatives showed turn-off fluorescence (Table 1) upon strong mechanical crushing and heating induced turn-on fluorescence (Table 1). Single crystal X-ray analysis revealed molecular conformational and packing change depending on the substituent and position that lead to tunable fluorescence. PXRD studies suggested the conversion of crystalline to amorphous and vice versa upon crushing and heating was responsible for fluorescence switching. Computational studies have been performed to get the insight on the energy level modulation upon changing of the molecular conformation.

Experimental Section

Triphenylamine, 3-methoxy-N,N-diphenylaniline, 4-methoxy triphenylamine, dimethylformamide (DMF, HPLC grade), phosphorous oxychloride, N-Methyl barbituric acid and indanedione were purchased from Sigma-Aldrich and used without further purification. Aldehyde functional group into triphenylamine, 3-methoxy triphenylamine and 4-methoxy triphenylamine was introduced by following reported procedure.[21]

General procedure for synthesizing N-Methylbarbituric acid derivatives (Scheme S1)

To the stirred solution of aldehyde (4-(diphenylamino)benzaldehyde/4-(diphenylamino)-2-methoxy benzaldehyde/4-((4-methoxyphenyl)(phenyl)amino) benzaldehyde) (1.0 equivalent) in methanol, 1.1 equivalents of N-methylbarbituric acid was added and stirred at room temperature for 6 hrs. The precipitated product from the reaction mixture was filtered and washed with cold methanol and dried.

5-(4-(diphenylamino)benzylidene)-1,3-dimethylpyrimidine-2,4,6(1H,3H,5H)-trione (BA-1)[22]

Bright yellow powder. Yield: 80%. M. p.: 190 °C, ^{1}H-NMR (300 MHz, $CDCl_3$) δ 8.43 (s, 1H), 8.23 (d, 2H), 7.39-7.34 (m, 4H), 7.26-7.19 (m, 6H), 6.94 (d, 2H), 3.41 (s, 3H), 3.38 (s, 3H). ^{13}C-NMR (75 MHz, $CDCl_3$) δ 163.56, 161.27, 158.37, 153.16, 151.61, 145.43, 138.05, 129.82, 126.73, 125.81, 124.55, 117.92, 112.25, 29.00, 28.31. LCMS (ESI) calcd. [M+]: 412.16, found: 412.2.

5-(4-(diphenylamino)-2-methoxybenzylidene)-1,3-dimethylpyrimidine-2,4,6(1H,3H,5H)-trione (BA-2).

Bright orange powder. Yield: 78%. M. p.: 227 °C, ^{1}H-NMR (300 MHz, $CDCl_3$) δ 8.98 (s, 1H), 8.58 (d, 1H), 7.39-7.34 (m, 4H), 7.23-7.19 (m, 6H), 6.51 (dd, 1H), 6.35 (d, 1H), 3.68 (s, 3H), 3.40 (s 3H), 3.36 (s, 3H). ^{13}C-NMR (75 MHz, $CDCl_3$) δ 163.80, 163.15, 161.42, 155.49, 152.74, 151.83, 145.53, 135.87, 129.74, 126.86, 125.82, 114.72, 111.43, 110.87, 99.83, 55.68, 28.85, 28.26. LCMS (ESI) calcd. [M+]: 442.17, found: 442.2.

5-(4-((4-methoxyphenyl)(phenyl)amino)benzylidene)-1,3-dimethylpyrimidine-2,4,6(1H,3H,5H)-trione (BA-3).

Bright orange red powder. Yield: 75%. M. p.: 150 °C, ^{1}H-NMR (300 MHz, $CDCl_3$) δ 8.42 (s, 1H), 8.23 (d, 2H), 7.38-7.33 (m, 2H), 7.22-7.13 (m, 5H), 6.94-6.86 (m, 4H), 3.83 (s, 3H), 3.41 (s, 3H), 3.38 (s, 3H). ^{13}C-NMR (75 MHz, $CDCl_3$) δ 163.66, 161.32, 158.38, 157.89, 153.35, 151.65, 145.37, 138.27, 138.05, 129.74, 128.58, 126.32, 125.64, 124.03, 116.99, 115.17, 111.74, 55.54, 28.98, 28.29. LCMS (ESI) calcd. [M+]: 442.17, found: 442.2.

General procedure for synthesizing indanedione derivatives (Scheme S2)

To the stirred solution of aldehyde (4-(diphenylamino) benzaldehyde/4-(diphenylamino)-2-methoxy-benzaldehyde/4-((4-methoxyphenyl)(phenyl)amino)benzaldehyde) (1.0 equivalent) in methanol, 1.1 equivalents of indanedione was added and stirred at room temperature for 6 hrs. The precipitated product from the reaction mixture was filtered and washed with cold methanol and dried.

2-(4-(diphenylamino)benzylidene)-1H-indene-1,3(2H)-dione (ID-1)

Bright orange red powder. Yield: 75%. M. p.: 221 °C, ^{1}H-NMR (300 MHz, $CDCl_3$) δ 8.42 (d, 2H), 7.97-7.92 (m, 2H), 7.78-7.74 (m, 3H), 7.39-7.34 (m, 4H), 7.23-7.19 (m, 6H), 7.01 (d, 2H). ^{13}C-NMR (75 MHz, $CDCl_3$) δ 191.29, 189.66, 152.72, 146.60, 145.75, 142.36, 139.97, 136.82, 134.79, 134.55, 129.77, 126.57, 125.74, 125.52, 125.31, 122.85, 122.82, 118.87. LCMS (ESI) calcd. [M+]: 402.14, found: 402.2.

2-(4-(diphenylamino)-2-methoxybenzylidene)-1H-indene-1,3(2H)-dione (ID-2)

Bright orange red powder. Yield: 80%. M. p.: 243 °C, ^{1}H-NMR (300 MHz, $CDCl_3$) δ 9.15 (d, 1H), 8.44 (s, 1H), 7.94-7.90 (m, 2H), 7.75-7.70 (m, 2H), 7.40-7.35 (m, 4H), 7.24-7.19 (m, 6H), 6.60 (dd, 1H), 6.40 (d, 1H), 3.71 (s, 3H). ^{13}C-NMR (75 MHz, $CDCl_3$) δ

View Article Online
DOI: 10.1039/C7CE01867C

191.71, 189.94, 162.77, 155.18, 145.65, 142.24, 140.58, 139.93, 136.03, 134.46, 134.25, 129.71, 126.75, 125.63, 124.03, 122.59, 115.56, 111.76, 100.52, 55.58. LCMS (ESI) calcd. [M+]: 432.16, found: 432.2.

2-(4-((4-methoxyphenyl)(phenyl)amino)benzylidene)-1H-indene-1,3(2H)-dione (ID-3)

Bright orange red powder. Yield: 82%. Melting point: 176 °C, ^{1}H-NMR (300 MHz, $CDCl_3$) δ 8.40 (d, 2H), 7.97-7.92 (m, 2H), 7.77-7.73 (m, 3H), 7.38-7.33 (m, 2H), 7.22-7.13 (m, 5H), 6.96-6.89 (m, 4H), 3.84 (s, 3H). ^{13}C-NMR (75 MHz, $CDCl_3$) δ 191.40, 189.70, 157.72, 153.08, 146.69, 145.70, 142.34, 139.95, 138.40, 136.97, 134.71, 134.45, 129.69, 128.51, 126.13, 125.30, 125.19, 124.87, 122.78, 122.75, 117.86, 115.15, 55.54. LCMS (ESI) calcd. [M+]: 432.16, found: 432.2.

Characterization

Fluorescence spectra and absolute quantum yield for all compounds in the solid state were recorded using Jasco fluorescence spectrometer-FP-8300 instruments equipped with integrating sphere and calibrated light source (D2 and W1). Powder X-ray diffraction (PXRD) patterns were measured using a XRD- Bruker D8 Advance XRD with Cu Kα radiation (λ = 1.54050 Å). Single crystals were coated with paratone-N oil and the diffraction data measured at 100K with synchrotron radiation (λ = 0.62998 Å) on a ADSC Quantum-210 detector at 2D SMC with a silicon (111) double crystal monochromator (DCM) at the Pohang Accelerator Laboratory, Korea. CCDC Nos. – 1579626-1579630 contain the supplementary crystallographic data for this paper. The HOMO, LUMO and band gap of all structures are studied using B3PW91/6-31+G(d,p) level theory (Gaussian 09 package).

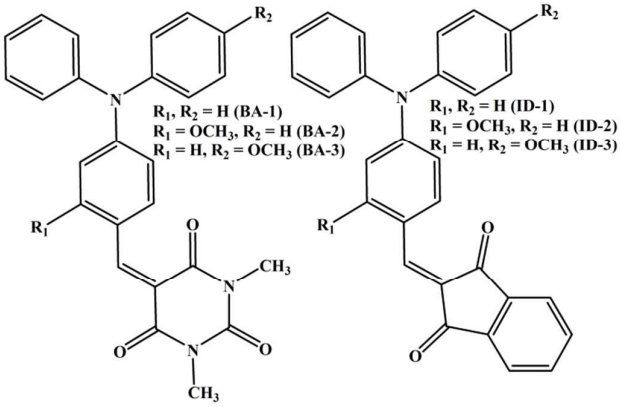

Chart 1. Molecular structure of BA and ID molecules.

Results and Discussion

Chart 1 shows the structures of TPA donor-π-acceptor derivatives based on N-methylbarbituric acid and indanedione. In solution, both BA-1-3 and ID-1-3 compounds showed only weak fluorescence (Fig. 1a, Table S1, Fig. S1). In contrast, both derivatives exhibited enhanced fluorescence in the solid state (Fig. 1b, Table 1, Table S1). The weak/non-fluorescence in solution and strong solid state fluorescence indicate the aggregation enhanced emission phenomena (AEE). TPA based donor-π-acceptor compounds are known to exhibit AEE phenomena.[20] Interestingly, BA-1-3 showed tunable fluorescence from yellow to red depend on the substitution position. The unsubstituted BA-1 showed strong yellow fluorescence whereas methoxy substitution at the phenyl ring

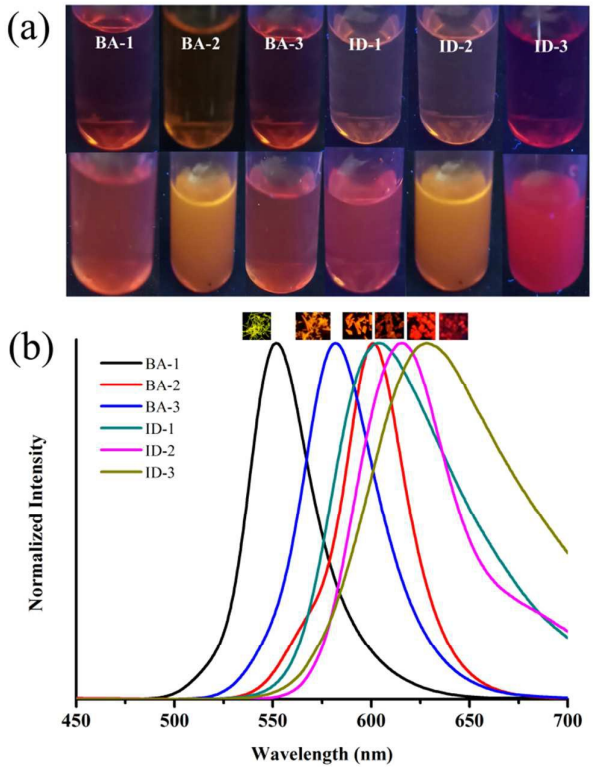

Fig. 1. BA and ID (a) digital fluorescence images in (I) CH_3CN and (II) water-CH_3CN mixture (95:5) and (b) solid state fluorescence spectra. The inset in (b) shows the digital fluorescence images of corresponding crystals. (λ_{exc} = 370 nm (spectra), 365 nm (digital images)).

Table 1. Absolute quantum yields of BA and ID derivatives.

	λ_{abs}, in CH_3CN (nm)	Crystals (%, Φ_f)	λ_{max} (nm)	Hard crushed (%, Φ_f)	λ_{max} (nm)	Heated (%, Φ_f)	λ_{max} (nm)
BA-1	458	22.8	550	3.1	530	14.5	530
BA-2	462	41.1	602	1.3	572	22.5	572
BA-3	468	19.1	582	1.3	557	7.7	557
ID-1	477	17.7	604	3.1	626	14.1	602
ID-2	482	19. 4	611	1.4	593	10.1	595
ID-3	488	14.1	636	1.2	650	10.0	606

in which acceptor is attached (BA-2) produced red fluorescence solids (Table 1). BA-3, in which methoxy group substituted at different phenyl ring of TPA, exhibited orange fluorescence (Table 1) in the solid state. BA-2 exhibited higher fluorescence intensity compared to BA-1 and 3 (Table 1). ID compounds showed tunable strong red fluorescence between 604 and 636 nm depend on the methoxy substitution position (Table 1). ID-2 exhibited higher fluorescence efficiency compared to ID-1 and 3 (Table 1). Slight breaking of BA crystals

View Article Online
DOI: 10.1039/C7CE01867C

showed blue shifting of fluorescence (Fig. 2, S1). However, both BA and ID compounds did not show significant change in the absorption in CH_3CN (Fig. S2). The crystals of BA-1 showed fluorescence at 550 nm that blue shifted to 541 nm upon slight breaking (Fig. S3a). Similarly slight breaking of BA-2 and BA-3 crystals also showed blue shifting of fluorescence from 602 to 573 nm (BA-2, Fig. 2a) and 582 to 570 nm (BA-3, Fig. S3b). Organic molecular materials are known to exhibit blue shift as well as strong enhancement of emission when the long range molecular ordering in the crystals was disturbed.[5a,20b,23] However, ID-1-3 did not show significant shift in the fluorescence λ_{max} upon slight breaking of crystals (Fig. 2b, S4). Importantly, the strong fluorescence of BA and ID compounds were completely turn-off by hard crushing (Fig. 2, 3, S3, S4, Table 1). BA-1 showed absolute quantum yield of (Φ_f) 22.8 % before crushing whereas after crushing it exhibited only 3.1%. BA-2 that showed highest fluorescence efficiency in the crystal and BA-3 also becomes weakly emissive solids after crushing (Table 1). Similarly, strongly fluorescent ID-1, ID-2 and BA-2 crystals also converted to weakly fluorescent solids by crushing. (Fig. 3, Table 1). Hard crushing of ID-1 showed red

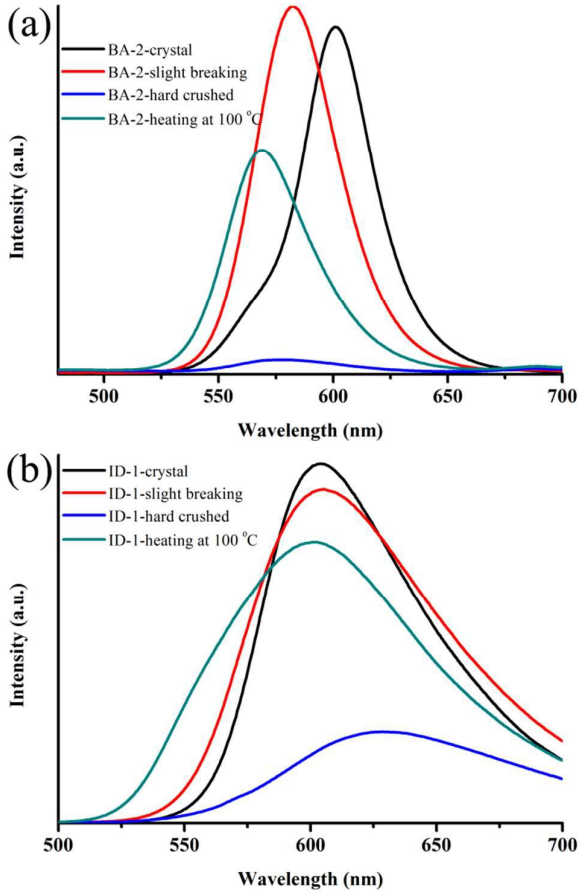

Fig. 2. Solid state fluorescence switching of (a) BA-2 and (b) ID-1 by external stimuli. (λ_{exc} = 370 nm).

shift of fluorescence (λ_{max} = 626 nm) with substantial reduction of intensity (Fig. 3). The mechanofluorochromism of ID-1 has already been reported.[24] ID-2 and ID-3 showed only reduction of fluorescence intensity without showing significant change of λ_{max}. The heating of hard crushed BA and ID solids exhibited turn-on fluorescence; though relatively low compared to initial fluorescence intensity (Fig. 2, 3, S3, S4, Table 1). After heating, both BA-1-3 and ID-1-3 crushed solids showed enhanced fluorescence intensity (Table 1). It is noted that crushed followed by heated BA solids showed blue shifted emission maximum compared to crystals/slightly broken crystals. This could be due to the disruption of the long range molecular ordering in the crystalline phase.[5a,20b,d,23] However, subsequent crushing and heating cycle did not show significant modulation in the emission maximum (Fig. S5). We have also prepared TPA based donor-acceptor dyes with barbituric acid without N-methyl to understand the role acceptor structure on the reversible fluorescence switching. Interestingly, the as synthesized TPA (DPBT-1) and 3-Methoxy TPA (DPBT-2) derivatives with barbituric acid showed red fluorescence at 602 nm (Φ_f = 12.3 and 13.6 %) and hard crushing completely quenched the fluorescence (Fig. S6). However, heating did not exhibit reversible turn-on fluorescence. This might be due to the strong intermolecular H-bonding capability of the barbituric acid via N-H...O interactions.[25] Thus N-methylation of nitrogen that prevents strong H-bonding network structure formation played important role on the reversible fluorescence switching.

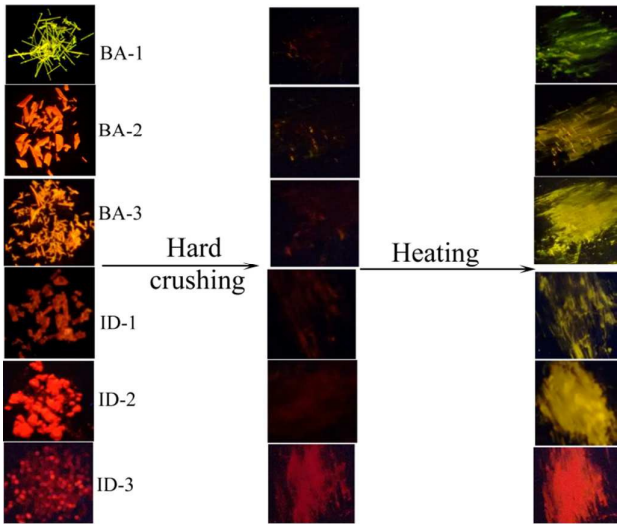

Fig. 3. Digital images of mechanofluorochromism of (a) BA and (b) ID compounds by hard crushing followed by heating. (λ_{exc} = 365 nm).

Single crystals of BA-1-3 and ID-1-3 were grown to get the insight on the molecular conformation and packing to understand the solid state fluorescence tuning and switching. Except ID-2, we were able to obtain good quality crystals of all other compounds by slow evaporation. In all the molecules TPA exhibited twisted molecular conformation. BA-1 showed H-bonding interaction between N-methylbarbituric acid carbonyl oxygen and phenyl hydrogen atoms of TPA and N-methylbarbituric acid carbon and nitrogen (Fig. 4). One of the carbonyl oxygen atom of N-methylbarbituric acid exhibited H-

View Article Online
DOI: 10.1039/C7CE01867C

bonding interaction with phenyl hydrogen atoms (Fig. 4a,b). Another carbonyl oxygen of N-methylbarbituric acid showed C=O…C and C=O…N interactions and these interactions lead to the formation of herringbone stacking structure in the crystal lattice (Fig. 4c). In contrast, BA-2 showed only H-bonding interaction between *para* carbonyl oxygen of N-methylbarbituric acid and phenyl hydrogen (Fig. 4d). The intermolecular interaction produced dimer that was further interconnected by H-bonding. However, BA-3 exhibited H-bonding and C=O…C and C=O…N interactions similar to BA-1 in the crystal lattice and produced similar herringbone structural arrangement (Fig. S7). It is noted that barbituric acid without methyl group on the nitrogen showed strong H-bonding with

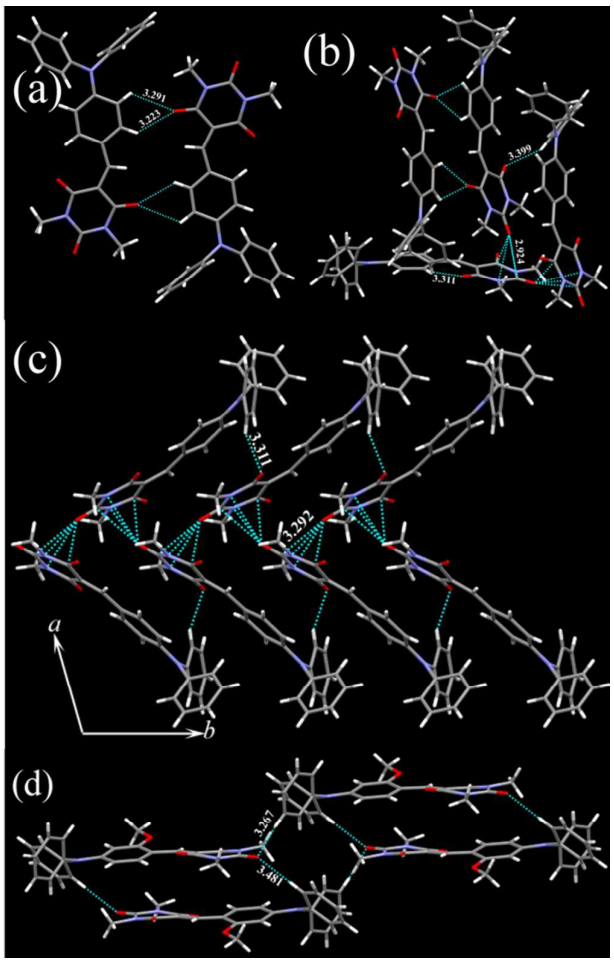

Fig. 4. (a)Dimer, (b) H-bonding interaction of other oxygen of N-methyl barbituric acid, (c) extended H-bonding interaction along b-axis in the crystal lattice of BA-1 and (d) H-bonding interaction in the crystal lattice of BA-2. C (grey), N (blue), O (red), H (white). H-bonding, C-O…π interactions (broken line) distances are marked in Å.

2D hexagonal network structure.[25] ID-1 showed dimer formation through H-bonding interactions between indanedione oxygen and phenyl hydrogen and π-π interactions between carbonyl and alkene further connects the dimer in the crystal lattice along *a*-axis (Fig. 5a). The H-bonding between oxygen and phenyl hydrogen of indanedione connects the network along *b*-axis (Fig. S8). ID-3 showed H-bonding interactions between methoxy oxygen and phenyl hydrogen and C-H…π interactions between phenyl hydrogen and indanedione (Fig. 5b, S9). The combined weak intermolecular interactions produced square structure in the crystal lattice. Figure 6 shows the comparison of molecular conformation of BA and ID molecules in the crystal lattice. The donor TPA phenyl group and acceptor N-methylbarbituric acid adopts coplanar conformation in BA-1 and BA-3 (Fig. 6a). Similarly, ID-1 also showed coplanar conformation between donor TPA phenyl group and acceptor indanedione. The coplanar conformation in BA-1, BA-3 and ID-1 produced strong intermolecular interactions with extended antiparallel dipole arrangement (H-aggregation) in the crystal lattice (Fig.

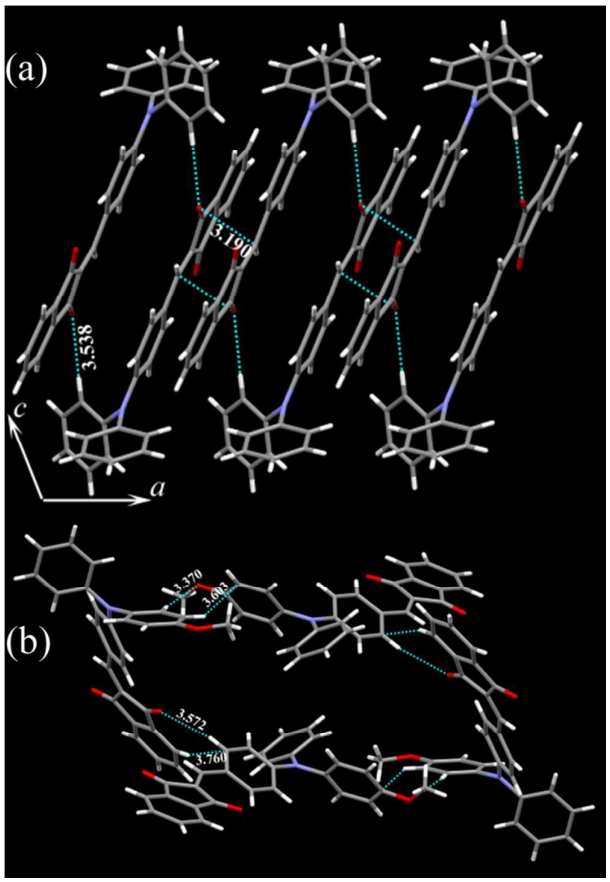

Fig. 5. (a) Dimer formation in ID-1 and (b) square structure formation in ID-2 via H-bonding interaction in the crystal lattice. C (grey), N (blue), O (red), H (white). H-bonding and C-O…π interactions (broken line) distances are marked in Å.

4,5a,S5). Whereas BA-2 and ID-3 exhibited twisted conformation between TPA phenyl donor and acceptor (N-methylbarbituric acid (BA-2) and indanedione (ID-3)). The twisted donor-acceptor conformation in BA-2 and ID-3 could increase the proportion of charge transfer states that lead to red shifting of fluorescence λ_{max}. The coplanar conformation with strong interactions might lead to blue shift of fluorescence λ_{max}. The superimposing of BA and ID structures revealed that TPA also adopted different conformation depend on the substitution and position of substitution (Fig. 6b,c).

View Article Online
DOI: 10.1039/C7CE01867C

However, the acceptors (N-methylbarbituric acid and indanedione) in both the derivatives did not show significant variation. The modulation of TPA conformation could also influence on the solid state fluorescence of TPA based donor-acceptor derivatives.[20]

The molecular conformational change induced optical band gap modulation and solid state fluorescence tuning was further supported by DFT calculations that were performed using single crystal structure of BA and ID (Fig. 7, S10, Table 2). The HOMO, LUMO and band gap of all structures are studied using B3PW91/6-31+G(d,p) level of theory. The isodensity surface plot (isodensity contour = 0.02) of the highest occupied molecular orbitals (HOMOs) of BA and ID indicated that electron density was predominantly localized on the TPA donor phenyl group and slightly over the acceptor. The electron density in the lowest unoccupied molecular orbitals (LUMOs) was mainly localized on the N-methylbarbituric acid and indanedione acceptor. The calculated band gap indicates that BA-2 showed lowest band gap of 3.03 eV compared to BA-1 and BA-3 (Table 2). ID-3 showed band gap of 2.78 eV

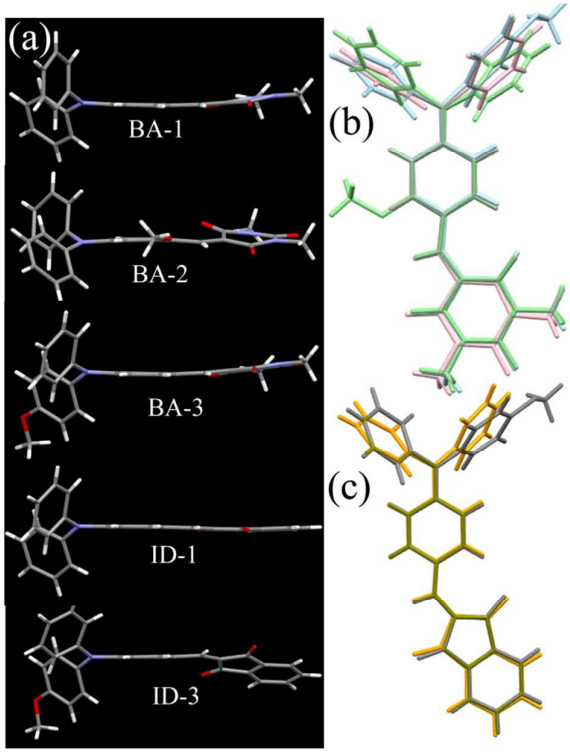

Fig.6. Molecular conformation of (a) BA and ID crystal lattice and superimposed images of (b) BA-1-3 and (c) ID-1 and 3. C (grey), N (blue), O (red), H (white). (BA-1 (pink), BA-2 (green), BA-3 (blue), ID-1 (orange) and ID-3 (grey).

compared to 3.00 eV of ID-1. The lower optical band gap leads to red fluorescence in BA-2 and ID compounds. Thus DFT calculation also supported the change of optical band gap due to the modulation of molecular conformation. To understand the mechanism of reversible fluorescence change of BA and ID compounds towards external stimuli, PXRD studies were performed before and after hard crushing as well as after heating (Fig. 8, S11,12). The initial compounds showed clear and strong diffraction peaks and confirmed the crystallinity of the sample. After hard crushing, the sharp diffraction peaks were disappeared or the intensity was substantially reduced (Fig. 8. S11,12). Hence hard crushing converted crystalline materials to amorphous phase or partially amorphous. However, heating of the hard crushed compounds showed

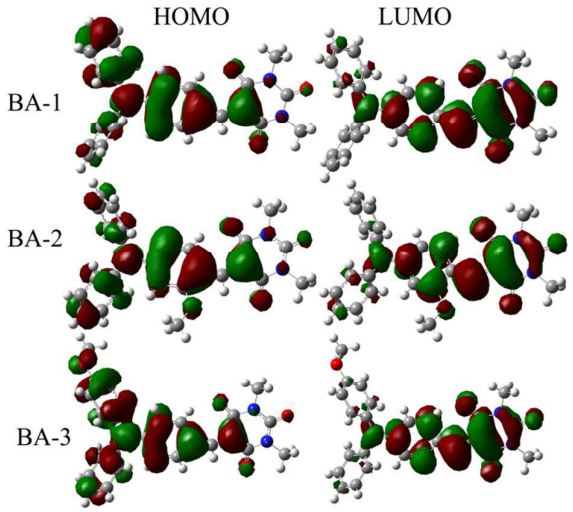

Fig. 7. Molecular orbital plots of the HOMOs and LUMOs of BA compounds.

Table 2.HOMO and LUMO energy levels of BA and ID derivatives.

Compound	HOMO (eV)	LUMO (eV)	Band gap (eV)
BA-1	-5.75	-2.52	-3.23
BA-2	-5.57	-2.55	-3.03
BA-3	-5.65	-2.41	-3.24
ID-1	-5.62	-2.62	-3.00
ID-3	-5.39	-2.61	-2.78

clear strong diffraction peaks that suggest the regeneration of crystalline phase from amorphous phase. DSC studies of crushed BA and ID compounds were also exhibited clear phase transition between 70 and 100 °C (Fig. S13,14). The matching of regenerated diffraction peaks after heating with the initial peaks position suggest that the compound did not undergo any structural change after crushing and heating. It is noted that hard crushed and heated BA-1 compounds showed some additional PXRD peaks compared to the initial crystals. However, the PXRD pattern of heated samples perfectly matched with the pattern generated using single crystal data (Fig. S15) and indicate that there is no structural change. Thus the off-on fluorescence switching of BA and ID was due to the reversible transformation of crystalline to amorphous and vice versa.

Conclusion

View Article Online
DOI: 10.1039/C7CE01867C

In conclusion, we have synthesized triphenylamine (TPA) and N-methylbarbituric acid/indanedione based donor-acceptor dye that exhibited molecular conformation and packing dependent tunable fluorescence from yellow to red in the solid state. The coplanar conformation between donor and acceptor in BA-1 and BA-3 showed bright yellow and orange fluorescence. The increasing electronic conjugation in BA-3 red shifted the fluorescence. Whereas strong twisting between donor and acceptor due to the steric effect caused by OCH_3 substituent in BA-2 produced strong red fluorescent solids. TPA with indanedione acceptor dyes exhibited red to deep red fluorescence (604 to 636 nm, Φ_f = 14.1 to 19.4 %). ID-1 showed coplanar conformation between donor and acceptor but increasing conjugation by indanedione led to red fluorescence. The strong twisting as well as increasing conjugation by OCH_3 substitution produced deep red fluorescence. Computational studies have been performed to get the insight on the energy level modulation upon changing of the molecular conformation. Importantly, both BA and ID derivatives showed off-on reversible fluorescence switching by hard crushing and heating. The studies of TPA with barbituric acid acceptor suggested N-methyl group played significant role on the reversible turn-on fluorescence while heating. PXRD studies revealed reversible conversion of crystalline to amorphous and amorphous to crystalline was responsible for fluorescence switching. Thus attachment of π-conjugated flat N-methylbarbituric acid and indanedione acceptor with TPA donor produced tunable, red fluorescent organic dyes that could exhibit external stimuli responsive high contrast reversible off-on fluorescence switching.

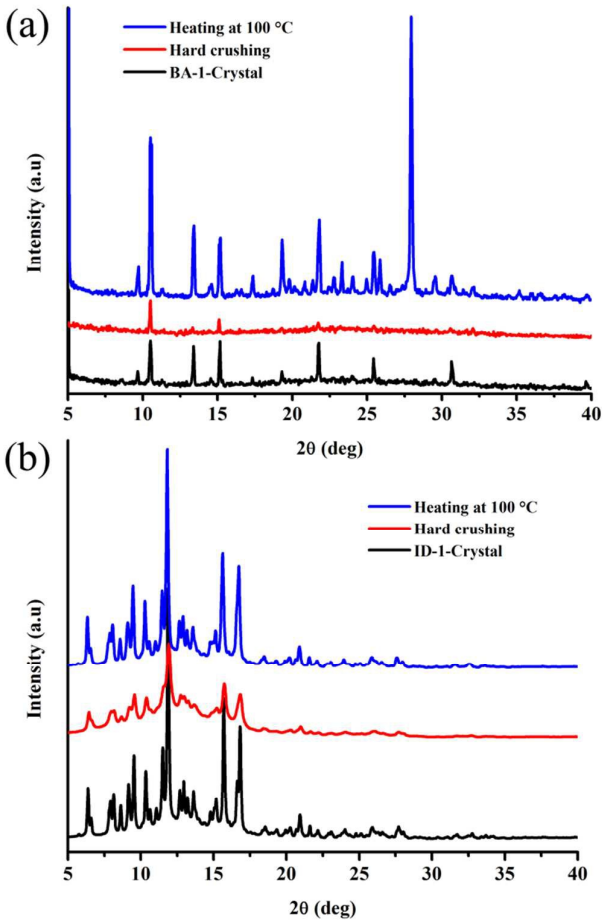

Fig. 8. PXRD pattern of (a) BA-1 and (b) ID-1 before, after hard crushing and heating.

Acknowledgement

Financial support from the Science and Engineering Research Board (SERB), New Delhi, India (SERB No. EMR/2015/00-1891) is acknowledged with gratitude. "X-ray crystallography at the PLS-II 2D-SMC beamline was supported in part by MSIP and POSTECH. DSC studies were supported by Basic Science Research Program through the National Research Foundation of Korea (NRF) funded by the Ministry of Education, Science and Technology (NRF-2017R1C1B2003111).

1 (a) S. Xu, H. Lu, X. Zheng, L. Chen, *J. Mater. Chem. C* 2013, **1**, 4406; (b) L. Xia, R. Xie, X. Ju, W. Wang, Q. Chen, L. Chu, *Nature Commun.*, 2013, **4**, 2226; (c) P. C. Xue, R. Lu, P. Zhang, J. Jia, Q. Xu, T. Zhang, M. Takafuji, H. Ihara, *Langmuir*, 2013, **29**, 417; (d) H. Ito, T. Saito, N. Oshima, N. Kitamura, S. Ishizaka, Y. Hinatsu, M. Wakeshima, M. Kato, K. Tsuge, M. Sawamura, *J. Am. Chem. Soc.*, 2008, **130**, 10044; (e) X. Q. Zhang, Z. G. Chi, Y. Zhang, S. W. Liu and J. R. Xu, *J. Mater. Chem. C*. 2013, **1**, 3376.

2 (a) S. Hirata and T. Watanabe, *Adv. Mater*. 2006, **18**, 2725; (b) S. Pucci, F. D. Cuia, F. Signori and G. Ruggeri, *J. Mater. Chem*. 2007, **17**, 783; (c) S. J. Lim, B. K. An, S. D. Jung, M. A. Chung and S. Y. Park, *Angew. Chem. Int. Ed.* 2004, **43**, 6346; (d) M. Shimizu and T. Hiyama, *Chem. Asian J*. 2010, **5**, 1516; (e) S. J. Toal, K. A. Jones, D. Magde and W. C. Trogler, *J. Am. Chem. Soc*. 2005, **127**, 11661; (f) C. E. Olson, M. J. R. Previte and J. T. Fourkas, *Nat. Mater*. 2002, **1**, 225; (g) A. Kishimura, T. Yamashita, K. Yamaguchi and T. Aida, *Nat. Mater*. 2005, **4**, 546.

3 (a) Z. G. Chi, X. Q. Zhang, B. J. Xu, X. Zhou, C. P. Ma, Y. Zhang, S. W. Liu and J. R. Xu, *Chem. Soc. Rev*., 2012, **41,** 3878; (b) P. -Z. Chen, H. Zhang, L. -Y. Niu, Y. Zhang, Y. –Z. Chen, H. –B. Fu and Q. –Z. Yang, *Adv. Funct. Mater*. 2017, **27**, 1700332; (c) L. Wang, K. Wang, B. Zou, K. Ye, H. Zhang and Y. Wang, *Adv. Mater.,* 2015, **27,** 2918; (d) S. P. Anthony, *ChemPlusChem*., 2012, **7,** 518; (e) P. Srujana and T. P. Radhakrishnan, *Angew. Chem. Int. Ed*., 2015, **54**, 7270; (g) S. P. Anthony, *Chem. Asian J.*, 2012, **7,** 374; (f) S. M. Draper and S. P. Anthony, *J. Phys. Chem. C*, 2010, **114,** 11708.

4 (a) J. Luo, Z. Xie, J. W. Y. Lam, L. Cheng, H. Chen, C. Qiu, H. S. Kwok, X. Zhan, Y. Liu, D. Zhu and B. Z. Tang, *Chem. Commun*., 2001, 1740; (b) B. -K. An, S. -K. Kwon, S. -D. Jung and S. Y. Park, *J. Am. Chem. Soc*., 2002, **124,** 14410; (c) J. Chen, C. C. W. Law, J. W. Y. Lam, Y. Dong, S. M. F. Lo, I. D. Williams, D. Zhu and B. Z. Tang, *Chem. Mater*., 2003, **15,** 1535; (d) G. Yu, S. Yin, Y. Liu, J. Chen, X. Xu, X. Sun, D. Ma, X. Zhan, Q. Peng, Z. G. Shuai, B. Z. Tang, D. B. Zhu, W. Fang and Y. Luo, *J. Am. Chem. Soc*., 2005, **127,** 6335; (e) S. Kim, S.–J. Yoon and S. Y. Park, *J. Am. Chem. Soc.* 2012, **134**, 12091.

5 (a) Y. Dong, B. Xu, J. Zhang, X. Tan, L. Wang, J. Chen, H. Lv, S.We, B. Li, L. Ye, B. Zou, W. Tian, *Angew. Chem. Int, Ed.*, 2012, **51**, 10782; (b) Y. Wang, W. Liu, L. Bu, J. Li, M. Zheng, D. Zhang, M. Sun, Y. Tao, S. Xue, W. Yang, *J. Mater. Chem. C*, 2013, **1**, 856; (c) S. Varghese, S. Das, *J. Phys. Chem. Lett*. 2011, **2**, 863; (d) G. Zhang, J. Lu, M. Sabat, C. L. Fraser, *J. Am. Chem. Soc*. 2010, **132**, 2160.

View Article Online
DOI: 10.1039/C7CE01867C

6 (a) P. Gautam, R. Maragani, M. M. Shaikh and R. Misra, *RSC Adv*. 2014, **4**, 52526; (b) R. H. Pawle, T. E. Haas, P. Müller and S. W. Thomas III, *Chem. Sci*. 2014, **5**, 4184; (c) Z. Zhang, D. Yao, T. Zhou, H. Zhang and Y. Wang, *Chem. Commun*. 2011, **47**, 7782; (d) L. Y. Bu, M. X. Sun, D. T. Zhang, W. Liu, Y. L. Wang, M. Zheng, S. F. Xue and W. J. Yang, *J. Mater. Chem. C*. 2013, **1**, 2028; (e) Y. Dong, J. W. Y. Lam, A. Qin, Z. Li, J. Sun, H. H.-Y. Sung, I. D. Williams and B. Z. Tang *Chem. Commun*. 2007, 40.

7 (a) S. Xu, Y. Yuan, X. Cai, C. J. Zhang, F. Hu, J. Liang, G. Zhang, D. Q. Zhang and B. Liu, *Chem. Sci*., 2015, **6,** 5824; (b) J. Huang, N. Sun, Y. Dong, R. Tang, P. Lu, P. Cai, Q. Q. Li, D. Ma, J. Qin and Z. Li, *Adv. Funct. Mater*., 2013, **23,** 2329; (c) G. Chen, W. Li, T. Zhou, Q. Peng, D. Zhai, H. Li, W. Z. Yuan, Y. M. Zhang and B. Z. Tang, *Adv. Mater*., 2015, **27,** 4496; (d) M. Huang, R. Yu, K. Xu, S. Ye, S. Kuang, X. Zhu and Y. Wan, *Chem. Sci*., 2016, **7,** 4485; (e) Z. M. Wang, H. Nie, Z. Q. Yu, A. J. Qin, Z. J. Zhao and B. Z. Tang, *J. Mater. Chem. C*, 2015, **3,** 9103; (f) Z. K. He, L. Q. Zhang, J. Mei, T. Zhang, J. W. Y. Lam, Z. G. Shuai, Y. Q. Dong and B. Z. Tang, *Chem. Mater*., 2015, **27,** 6601.

8 (a) J. A. Delaire and K. Nakatani, *Chem. Rev*., 2000, **100,** 1817; (b) H. Tian and S. J. Yang, *Chem. Soc. Rev*., 2004, **33,** 85; (c) T. Yamase, *Chem. Rev*., 1998, **98,** 307; (d) M. Irie, T. Fukaminato, T. Sasaki, N. Tamai and T. Kawai, *Nature*, 2002, **420,** 759; (e) M. Koenig, B. Storti, R. Bizzarri, D. M. Guldi, G. Brancato and G. Bottari, *J. Mater. Chem. C*, 2016, **4,** 3018; (f) Z. Ma, Z. Wang, X. Meng, Z. Ma, Z. Xu, Y. Ma and X. Jia, *Angew. Chem. Int. Ed.*, 2016, **55,** 519; (g) S. Yagai, S. Okamura, Y. Nakano, M. Yamauchi, K. Kishikawa, T. Karatsu, A. Kitamura, A. Ueno, D. Kuzuhara, H. Yamada, T. Seki and H. Ito, *Nat. Commun*., 2014, **5,** 4013; (h) S. -J. Yoon, J. W. Chung, J. Gierschner, K. S. Kim, M. -G. Choi, D. Kim and S. Y. Park, *J. Am. Chem. Soc*., 2010, **132,** 13675; (i) J. Kunzelman, M. Kinami, B. R. Crenshaw, J. D. Protasiewicz and C. Weder, *Adv. Mater*. 2008, **20,** 119; (j) T. Butler, W. A. Morris, J. Samonina-Kosicka and C. L. Fraser, *ACS Appl. Mater. Interfaces*, 2016, **8,** 1242; (k) Z. Zhang, Z. Wu, J. Sun, B. Yao, G. Zhang, P. Xue and R. Lu, *J. Mater. Chem. C,* 2015, **3,** 4921.

9 (a) Z. Zhao, S. Chen, J. W. Y. Lam, Z. Wang, P. Lu, F. Mahtab, H. H. Y. Sung, I. D. Williams, Y. Ma, H. S. Kwok and B. Z. Tang, *J. Mater. Chem*. 2011, **21**, 7210; (b) G.- F. Zhang, M. P. Aldred, W.- L. Gong, C. Li and M.- Q. Zhu, *Chem. Commun*. 2012, **48**, 7711; (c) H. G. Lu, B. Xu, Y. J. Dong, F. P. Chen, Y. W. Li, Z. F. Li, J. T. He, H. Li, W. J. Tian, *Langmuir.* 2010, **26**, 6838; (d) Z. Ning, Z. Chen, Q. Zhang, Y. Yan, S. Qian, Y. Cao and H. Tian, *Adv. Funct. Mater*. 2007, **17**, 3799; (e) G. Fan and D. Yan, *Scientific Reports*. 2014, **4**, 4933.

10 (a) J. Yang, Z. Ren, Z. Xie, Y. Liu, C. Wang, Y. Xie, Q. Peng, B. Xu, W. Tian, F. Zhang, Z. Chi, Q. Li and Z. Li, *Angew. Chem. Int. Ed.,* 2016, **55,** 1.

11 (a) Q. Song, Y. Wang, C. Hu, Y. Zhang, J. Sun, K. Wang and C. Zhang, *New J. Chem*., 2015, **39,** 659.

12 (a) X. Luo, J. Li, C. Li, L. Heng, Y. Q. Dong, Z. Liu, Z. Bo and B. Z. Tang, *Adv. Mater*., 2011, **23,** 3261; (b) Y. Zhao, H. Gao, Y. Fan, T. Zhou, Z. Su, Y. Liu and Y. Wang, *Adv. Mater*., 2009, **21,** 3165; (c) Y. Sagara, K. Kubo, T. Nakamura, N. Tamaoki and C. Weder, *Chem. Mater.,* 2017, **29,** 1273*;* (d) A. Lavrenova, D. W. R. Balkenende, Y. Sagara, S. Schrettl, Y. C. Simon and C. Weder, *J. Am. Chem. Soc*., 2017, **139,** 4302; (e) X. Chen, X. Zhang and G. Zhang, *Chem. Commun*., 2015, **51,** 161.

13 J. Kunzelman, M. Kinami, B. R. Crenshaw, J. D. Protasiewicz, C. Weder, *Adv. Mater*. 2008, **20**, 119.

14 (a) J. Luo, L. Y. Li, Y. L. Song and J. Pei, *Chem. Eur. J*. 2011, **17**, 10515; (b) M. J. Teng, X. R. Jia, S. Yang, X. F. Chenand, Y. Wei, *Adv. Mater*. 2012, **24**, 1255; (c) Y. J. Zhang, J. W. Sun, X. J. Lv, M. Ouyang, F. Cao, G. X. Pan, L. P. Pan, G. B. Fan, W. W. Yu, C. He, S. S. Zheng, F. Zhang, W. Wang and C. Zhang, *CrystEngComm*. 2013, **15**, 8998; (d) Anu Kundu, P. S. Hariharan, K. Prabakaran, D. Moon and S. P. Anthony, *RSC Adv*., 2015, **5**, 98618.

15 M. S. Kwon, J. Gierschner, S. J. Yoon and S. Y. Park, *Adv. Mater*. 2012, **24**, 5487.

16 R. M. Rao, C. W. Liao, W. L. Su and S. S. Sun, *J. Mater. Chem. C*. 2013, **1**, 5491.

17 C. Feng, K. Wang, Y. Xu, L. Liu, B. Zou and P. Lu, *Chem. Commun*., 2016, **52,** 3836.

18 (a) Y. Lei, Y. Liu, Y. Guo, J. Chen, X. Huang, W. Gao, L. Qian, H. Wu, M. Liu and Y. Cheng, *J. Phys. Chem. C*, 2015, **119,** 23138; (b) P. Xue, P. Chen, J. Jia, Q. Xu, J. Sun, B. Yao, Z. Zhang and R. Lu, *Chem. Commun*., 2014, **50,** 2569; (c) Y. Gong, Y. Tan, J. Liu, P. Lu, C. Feng, W. Z. Yuan, Y. Lu, J. Z. Sun, G. He and Y. Zhang, *Chem. Commun*., 2013, **49,** 4009; (d) H. N. Tian, X. C. Yang, J. X. Pan, R. K. Chen, M. Liu, Q. Y. Zhang, A. Hagfeldt and L. C. Sun, *Adv. Funct. Mater.*, 2008, **18,** 3461; (e) A. Mishra, M. K. R. Fischer and P. Bäuerle, *Angew. Chem. Int. Ed*., 2009, **48,** 2474.

19 (a) Z. Zhang, Z. Wu, J. Sun, B. Yao, P. Xuea and R. Lu, *J. Mater. Chem. C*, 2016, **4,** 2854; (b) M. Ouyang, L. Zhan, X. Lv, F. Cao, W. Li, Y. Zhang, K. Wang and C. Zhang, *RSC Adv*., 2016, **6,** 1188; (c) Y. Cao, W. Xi, L. Wang, H. Wang, L. Kong, H. Zhou, J. Wu and Y. Tian, *RSC Adv*., 2014, **4,** 24649.

20 (a) P. S. Hariharan, N. S. Venkataramanan, D. Moon and S. P. Anthony, *J. Phys. Chem. C*, 2015, **119,** 9460; (b) P. S. Hariharan, D. Moon and S. P. Anthony, *J. Mater. Chem. C*, 2015, **3,** 8381; (c) P. S. Hariharan, E. M. Mothi, D. Moon and S. P. Anthony, *ACS Appl. Mater. Interfaces*, 2016, **8,** 33034; (d) P. S. Hariharan, V. K. Prasad, S. Nandi, A. Anoop, D. Moon and S. P. Anthony, *Cryst. Growth Des.*, 2016, **17,** 146; (e) P. S. Hariharan, D. Moon and S. P. Anthony, *CrystEngComm*., 2017, DOI: 10.1039/C7CE01650F.

21 (a) Y. Li, L. Xue, H. Xia, B. Xu, S. Wen, W. Tian, *J. of Polymer Sci: Part A: Polymer Chem.* 2008, **46**, 3970.

22 S.-H. Kim, Y.-S. Kim, D.-H. Lee and Y.-A. Soni, *Mol. Cryst. Liq. Cryst*., 2011, **550**, 240.

23 (a) T. Han, Y. Hong, N. Xie, S. Chen, N. Zhao, E. Zhao, J. W. Y. Lam, H. Y. Sung, Y. Dong, B. Tong and B. Z. Tang, *J. Mater. Chem. C*, 2013, **1**, 7314; (b) S. Ito, T. Yamada, and M. Asami, *ChemPlusChem.* 2016, **81**, 1272; (c) Z. Lin, X. Mei, E. Yang, X. Li, H. Yao, G. Wen, C.-T. Chien, T. J. Chow and Q. Ling, *CrystEngComm*. 2014, **16**, 11018.

24 C. Qi, H. Ma, H. Fan, Z. Yang, H. Cao, Q. Wei, and Z. Lei, *ChemPlusChem*. 2016, **81**, 637.

25 (a) R. Misra, T. Jadhav, B. Dhokale and S. M. Mobin, Chem. Commun., 2014, **50**, 9076; (b) R. Li, S. Xiao, Y. Li, Q. Lin, R. Zhang, J. Zhao, C. Yang, K. Zou, D. Li and T. Yi, Chem. Sci., 2014, **5**, 3922.

View Article Online
DOI: 10.1039/C7CE01867C

Graphical Abstract

Synthesis of tunable, red fluorescent aggregation enhanced emissive organic fluorophores: Stimuli responsive high contrast off-on fluorescence switching

Molecular conformation controlled tunable fluorescence and stimuli responsive high contrast off-on high contrast off-on mechanofluorochromism has been demonstrated.